IFSCC 2025 full paper (IFSCC2025-450)

Study on the anti-aging effect of a composite nanocarrier with regulation of autophagy and inhibition of oxidative stress

Lingling Jiang[1], Min Liu[1#], Lei Ye[1], Cui Sun[1], Jiuyan Zheng[1]

[1] Suzhou MISIFU Cosmetics Co., Ltd, suzhou, China
[#] Corresponding author and presenting author

Abstract

Ribose / Collagen / Decarboxy Carnosine HCL / Palmitoyl Tripeptide-1 Composite Nanocarriers (RCDP NCs) were prepared by transdermal drug delivery nanotechnology. The safety of RCDP NCs was tested by cytotoxicity and patch test. Skin penetration was observed using laser confocal microscope. The uptake behavior of RCDP NCs by skin fibroblasts (HSF) and skin keratinocytes (HaCaT) was detected via laser confocal microscopy and flow cytometry. The anti-aging effects of RCDP NCs were investigated by measuring ROS fluorescence intensity detection and performing β-galactosidase staining on HSF cells in proliferation and oxidative damage model. Autophagy effect of RCDP NCs was studied using MDC fluorescence detection,transmission electron microscopy observation of autophagosomes and autophagy-related protein expression experiments. The results showed that RCDP NCs were safe and had no skin irritation. They enhanced percutaneous penetration of encapsulated components, improved cellular uptake, and promoted cell proliferation. RCDP NCs significantly reduced the content of ROS and MDA in oxidatively damaged cells. In addition, RCDP NCs can reduce the expression of P62 protein, increase the ratio of LC3II / LC3I protein expression, and increase the average fluorescence intensity of MDC specifically labeled autophagosomes, thereby increasing the number of autophagosomes. These findings suggest that RCDP NCs is an anti-aging raw material with high safety, good permeability, and can be taken up and utilized by skin cells. It can inhibit oxidative stress and regulate autophagy to delay skin aging, and its anti-aging effect is better than its free components.

Key words: composite nanocarriers; percutaneous penetration; cell uptake; anti-aging; autophagy

1. Introduction

As human longevity increases and societies age, public interest in aesthetics has grown. Understanding the mechanisms of skin aging and ways to slow it down has become a key focus in cosmetic research [1]. The complexity of skin aging involves multiple mechanisms; therefore, a single approach cannot effectively address all signs of aging [2]. A thorough investigation into these mechanisms, along with the development of skincare products targeting multiple pathways, can lead to more effective anti-aging ingredients.

The accumulation of free radicals causes oxidative stress that can damage lipids, proteins, nucleic acids, and organelles. This buildup of non-functional or damaged components compromises cellular integrity and promotes senescence [3,4]. Autophagy helps maintain intracellular balance under stress conditions as a survival mechanism against both internal and external threats [5]. However, cellular senescence is associated with reduced autophagic activity, which allows further accumulation of damaged components that hastens

senescence. Therefore, moderate activation and regulation of autophagy can help delay this process beneficially [6].

Ribose can improve cellular energy supply and promote autophagy [7-9]. Recombinant human collagen III (collagen) is a functional fragment from human collagen III with high activity and notable transdermal performance. Its curved triple helical structure facilitates superior adhesion to melanocytes, fibroblasts, macrophages, and other cell types, enhancing cellular attachment [10,11]. Decarboxy carnosine HCL exhibits multiple functions, including anti-oxidation, anti-glycation [12]. Palmitoyl tripeptide-1 promotes extracellular matrix synthesis of collagen and glycosaminoglycans [13].

In cosmetic or transdermal drug delivery formulations, nanocarriers significantly improve the skin penetration of active ingredients. By simultaneously encapsulating multiple distinct active components within a single nanocarrier, sustained release, prolonged efficacy, and synergistic effects are achieved through multi-target mechanisms, greatly enhancing overall effectiveness [14-16]. This research focused on RCDP NCs, which incorporate ribose, collagen, decarboxy carnosine, and palmitoyl tripeptide-1. Free RCDP was used as a control to evaluate the transdermal penetration, cellular uptake, antioxidative capacity, anti-aging effects, and autophagic regulation of RCDP NCs.

2. Material and Methods

2.1. Materials and Reagents

Bama pig skin, Zhifu District Yourong. HaCaT and HSF, Kunming Cell Bank, Chinese Academy of Sciences. Recombinant human collagen Ⅲ, Shanxi Jinbo. Dulbecco's modified eagle medium (DMEM), trypsin, double antibody, fetal bovine serum, and phosphate buffered saline (PBS), Gibco. Cell Counting Kit-8 (CCK-8), ROS detection kit, β-galactosidase staining kit, and MDA detection kits, Beyotime. Bicinchoninic acid protein concentration assay kit, glyceraldehyde-3-phosphate dehydrogenase (GAPDH) primary antibody, microtubule-associated protein 1 light chain 3 (LC3) primary antibody, Sequestosome-1 (P62) primary antibody and horseradish peroxidase-conjugated affinipure goat anti-rabbit IgG (H&L), Sevier. All other reagents, Sinopharm Group. The BB150 carbon dioxide cell incubator, Thermo Fisher Scientific. The SW-CJ-2FD ultra-clean worktable, Suzhou Purification Equipment. The Zetasizer/Nano-ZS90 Particle Size Analyzer, Malvern. The multi-label microplate reader, Perkin Elmer. The FV3000 laser confocal microscope, Olympus. Flow cytometer, Beckman. The MF52-N inverted microscope, Guangzhou Mingmei. The CT15RE desktop high-speed refrigerated centrifuge and HT7700 transmission electron microscope. The WB electrophoresis apparatus and chemiluminescence imaging system, Servicebio.

2.2. Preparation method of RCDP NCs

To prepare 1,000.0 g of RCDP NCs, the following components were accurately weighed: 20.0 g of ribose, 0.3 g of palmitoyl tripeptide-1, 100.0 g of glycerol, 150.0 g of pentylene glycol, 100.0 g of ethoxydiglycol, 100.0 g of polysorbate 80, 100.0 g of PEG-40 hydrogenated castor oil, and 30.0 g of lecithin. These were stirred at 55 °C to form a homogeneous solution A. In another container, a mixture was prepared by weighing and stirring together: 10.0 g of decarboxy carnosine HCl, 1.0 g of collagen, 5.0 g of sodium bisulfite, and 383.7 g of water at the same temperature to create solution B. Solution A was gradually added to solution B under continuous stirring at 55 °C until a uniform mixed solution C was obtained.This final mixture was homogenized twice in a high-pressure homogenizer at 850 bar to produce RCDP NCs with bilayer vesicles. Measure the particle size, PDI, and zeta potential of 0.1 g/mL RCDP NCs.

2.3. Percutaneous penetration

Rhodamine B (RhoB) was used as a fluorescent marker to prepare rhodamine B composite nanocarriers (RhoB NCs), alongside an equivalent concentration (0.20 g/L) of free RhoB solution. RhoB NCs were prepared following the same methodology as RCDP NCs. Panama pig-isolated skin was placed between the receiving and supply chambers of a diffusion cell.

Then, 0.5 g of RhoB NCs essence (5% RhoB NCs) and Free RhoB essence (with equivalent RhoB concentration) were applied to the supply chamber, while PBS served as the receptor solution. After 2 and 4 hours, residual samples were erased, target skin areas excised, rinsed, and frozen for sectioning. Laser confocal microscopy was used for detection, and ImageJ software quantified fluorescence signals to assess penetration depth and intensity.

2.4. The uptake of RCDP NCs by cells

HaCaT cells and HSF cells were seeded at densities of 2.0×10^5 and 1.6×10^5 cells per dish, respectively. After 24 h, DMEM containing Free RhoB or RhoB NCs was added for incubation periods of 2 h and 4 h. Following incubation, the medium was removed, and cells were washed three times with PBS, fixed with paraformaldehyde, and stained with DAPI for 15 min. Observations were made under a 60-fold objective using laser confocal microscopy. Cellular uptake was quantitatively assessed via flow cytometry. Follow the same inoculation and incubation procedures as in the previous experiment. After the cultivation, cell pellets were harvested, resuspended in cold PBS (0.5 mL), and mean fluorescence intensity within the cells was measured via flow cytometry.

2.5. β-galactosidase staining observation

HSF cells(passage 15) were seeded with density of 1.6×10^5 cells per well. After 24 h, the control group received DMEM, while sample groups were treated with DMEM containing either RCDP NCs (400 mg/L) or Free RCDP. After 48 h of cultivation, cells were washed 3 times with PBS. Subsequently, each well was treated with 1.0 mL of β-galactosidase staining fixative for 15 minutes at room temperature, followed by three washes with PBS. Next, 1.0 mL of β-galactosidase staining working solution was added to the samples, which were then incubated overnight at 37 °C. Staining results were visualized under a microscope.

2.6. Evaluation of ROS with fluorescent probe

HSF cells were seeded in 24-well plates at a density of 4×10^4 cells per well with 500 μL of medium. After 24 h, the supernatant was discarded. The model group received DMEM containing 0.6 mmol/L H_2O_2, while other sample groups received DMEM with 0.6 mmol/L H_2O_2 and varying concentrations of samples; a control group without H_2O_2 was included. After an additional 24 h, DMEM containing 20 μmol/L of 2,7-dichlorofluorescein diacetate was added and incubated for 20 minutes. Cells were washed three times with PBS, and fluorescence intensity was measured by flow cytometry. The experimental concentration of RCDP NCs was set at 400 mg/L, with Free RCDP prepared at an equivalent concentration.

2.7. Lipid peroxidation product MDA

HSF cells underwent the same incubation and administration procedures as described in the previous experiment, followed by a 24-hour culture period post-treatment. Intracellular malondialdehyde (MDA) levels were quantified according to the assay kit manufacturer's instructions.

2.8. Autophagy-related protein

HSF cells were seeded in 10 mm culture dishes at a density of 8×10^5 cells per dish with 10 mL of medium. After 24 h, the supernatant was removed and replaced with complete DMEM containing either 400 mg/L or 800 mg/L of RCDP NCs or Free RCDP (at equivalent concentrations of functional components). The cells were then cultured for another 48 h. Cellular proteins were extracted using a protein lysis buffer, and their concentrations were quantified using a bicinchoninic acid assay kit. For SDS-PAGE analysis, 60 μg of protein per lane was loaded onto a polyacrylamide gel. Following electrophoresis, proteins were transferred to polyvinylidene fluoride membranes using a semi-dry transfer system. The membranes were incubated overnight at 4 °C with primary antibodies against P62, LC3I, LC3II, and GAPDH at appropriate dilutions. After three washes with Tris-buffered saline containing Tween-20, horseradish peroxidase (HRP)-conjugated goat anti-rabbit secondary antibody was applied. A chemiluminescence solution (1:1 ratio) was prepared and evenly applied to the membrane on the exposure plate. Images were captured and analyzed using an automated fluorescence/visible light gel imaging system.

2.9. Autophagosomes

The incubation procedures for HSF cells were the same as in the previous experiment. After 24 h, the supernatant was removed and replaced with DMEM complete medium containing 400 mg/L of either RCDP NCs or Free RCDP. The cells were cultured for an additional 48 h before being harvested using trypsin digestion and centrifugation until aggregation occurred. The resulting cellular pellet was dissociated and fixed with 2.5% glutaraldehyde in phosphoric acid buffer, then stored at 4 °C overnight. After multiple rinses with PBS, specimens were post-fixed with 1% osmium tetroxide for 1-2 h. Cellular samples underwent gradient dehydration through increasing concentrations of ethanol and acetone, followed by embedding, sectioning, and examination for autophagic structures via transmission electron microscopy.

2.10. Monodansylcadaverine (MDC) staining

HSF cells were seeded into 10 mm cell culture dishes at a density of 8×10^4 cells per dish, with 2.0 mL of medium added to each dish. After 24 h of culture, the supernatant was discarded. Then, DMEM containing 400 mg/L RCDP NCs and the free component solution was added to the dishes, and the cells were cultured for an additional 48 h. Subsequently, the cells were rinsed once with PBS, incubated at 37 °C for 4 h, and rinsed once again with PBS. Next, 1 mL of 50 μmol/L MDC was added per well, and the cells were incubated at room temperature in the dark for 30 minutes. Finally, the cells were rinsed three times with PBS, and the fluorescence intensity was detected by flow cytometry.

3. Results

3.1. Particle size, PDI and Zeta potential

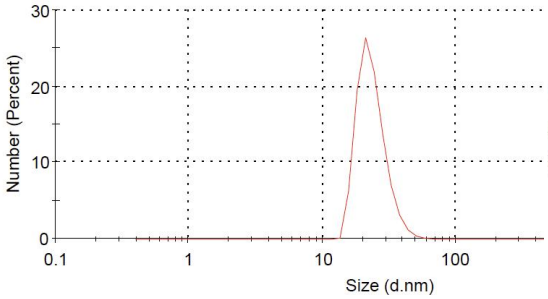

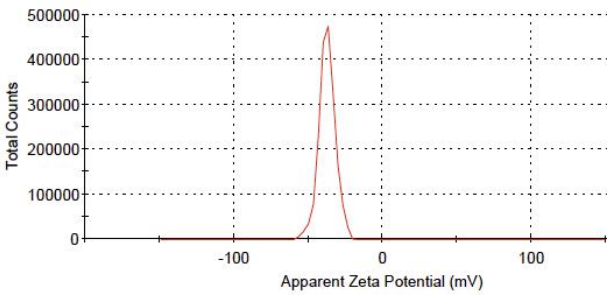

Figure 1. Size distribution by number of RCDP NCs. **Figure 2.** *Zeta potential distribution of RCDP NCs.*

The RCDP NCs was a light yellow transparent liquid. They were characterized by a mean particle size of 33.1 nm, a PDI of 0.292, and a Zeta potential of (-34.2 ± 0.7) mV. As illustrated in Figure 1, the size distribution by number exhibits a narrow range, indicating uniform vesicle dimensions, with nearly all particles measuring below 50 nm in diameter. Figure 2 demonstrates a narrow Zeta potential distribution range, with vesicle surfaces predominantly bearing negative charges, thereby confirming the stability of the RCDP NCs.

3.2. In vitro skin penetration

To evaluate the dermal penetration capability of RCDP NCs, RhoB was encapsulated within the nanocarriers, and both penetration depth and fluorescence intensity were assessed at various time intervals using the vertical Franz diffusion cell methodology. The experimental outcomes are presented in Figure 3, after 2 h, Free RhoB was mainly confined to the stratum corneum and was unable to penetrate this barrier. In contrast, RhoB NCs effectively crossed the stratum corneum within the same period. After 4 h, the fluorescence penetration depth of RhoB NCs increased significantly, reaching 460.0 μm. Furthermore, both the fluorescence intensity and penetration depth of RhoB NCs were markedly higher than those of Free RhoB. These results indicate that nanocarriers enhance the rapid and effective delivery of encapsulated components to deeper dermal tissues.

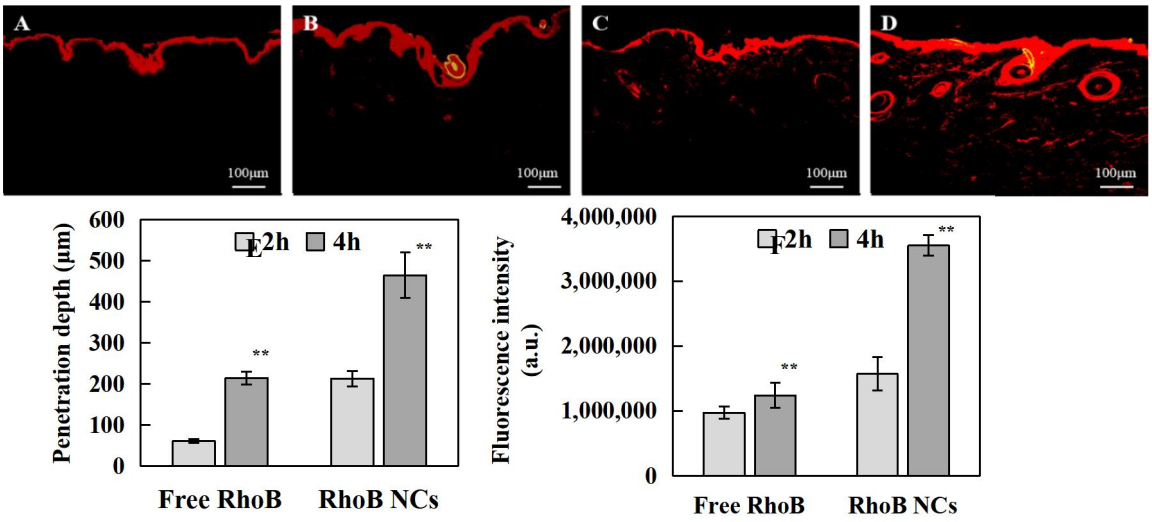

Figure 3. Percutaneous penetration: A. Free RhoB permeation for 2 h (10X); B. Free RhoB permeation for 4 h (10X); C. RhoB NCs permeation for 2 h (10X); D. RhoB NCs permeation for 4 h (10X); E. Penetration depth; F. Fluorescence intensity. (Note: Compared with Free RhoB, **P < 0.01.)

3.3. Cell proliferation

The proliferative effects of Free RCDP and RCDP NCs on HaCaT and HSF cells are presented in Figure 4.

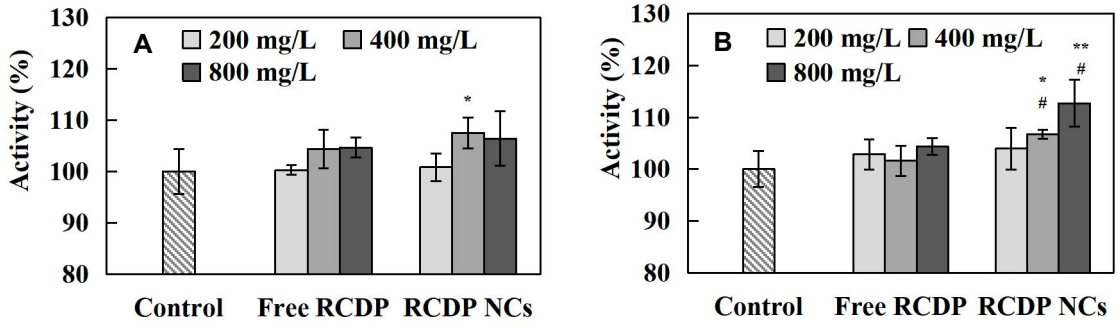

Figure 4. A. Effect of Free RCDP and RCDP NCs on the proliferation of HaCaT cells; B. Effect of Free RCDP and RCDP NCs on the proliferation of HSF cells. (Note: Compared with the Control group, **P < 0.01, *P < 0.05; compared with the same concentration of Free RCDP, # P < 0.05.)

As depicted in Figure 4A, RCDP NCs at a concentration of 400 mg/L significantly enhanced the proliferation of HaCaT cells compared with the Control group. Figure 4B demonstrates that RCDP NCs at concentrations of 400 mg/L and 800 mg/L markedly stimulated HSF cell proliferation compared with the Control group. When compared with Free RCDP, HSF cell proliferation was significantly increased at RCDP NCs concentrations of 400 mg/L and 800 mg/L.

3.4. The uptake of RCDP NCs by cells

To evaluate whether RCDP NCs can effectively deliver functional components into HaCaT and HSF cells, it was deemed essential to investigate the cellular entry behavior of the nanocarrier-encapsulated components [17]. According to Figure 5, the fluorescence intensity in HaCaT and HSF cells significantly increased with prolonged incubation time. Compared to the free RhoB group, the average fluorescence intensity in HaCaT cells treated with RhoB nanocapsules was enhanced by 53.73% and 47.37% at 2 and 4 h, respectively. Similarly, the average fluorescence intensity in HSF cells treated with RhoB nanocapsules increased by 27.60% and 89.11% at 2 and 4 h, respectively. These results confirm that RCDP nanocapsules effectively deliver encapsulated bioactive substances to target skin cells.

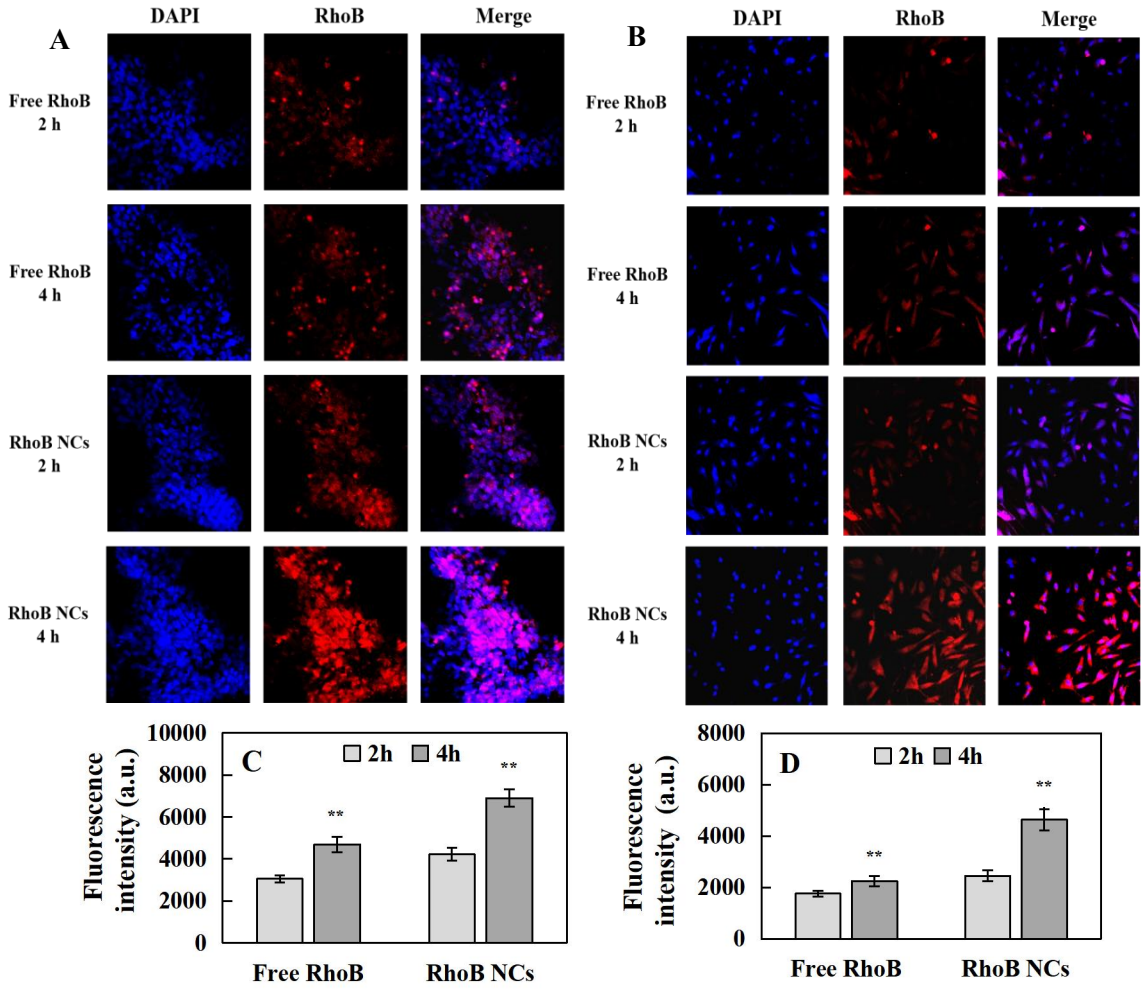

Figure 5. Cell uptake: A. Uptake by HaCaT cells (60X); B. Uptake by HSF cells (60X); C. Quantitative analysis of HaCaT cell uptake; D. Quantitative analysis of HSF cell uptake. (Note: Compared with Free RhoB, **P < 0.01.)

3.5. cellular oxidative stress

Oxidative stress is widely recognized as a primary contributor to skin aging. The effects of Free RCDP and RCDP NCs on oxidative parameters in the oxidized cell model are shown in Figure 6.The average fluorescence intensity of ROS was 8605 in model group, which was higher than that in control group. Compared with model group, ROS intensity significantly decreased in both the free component and RCDP NCs groups. 400 mg/L of RCDP NCs further reduced ROS levels compared to free components. Free RCDP at 800 mg/L and RCDP NCs at 400 mg/L and 800 mg/L significantly reduced MDA levels compared to the model group. Additionally, RCDP NCs at both concentrations exhibited lower MDA content than Free RCDP.

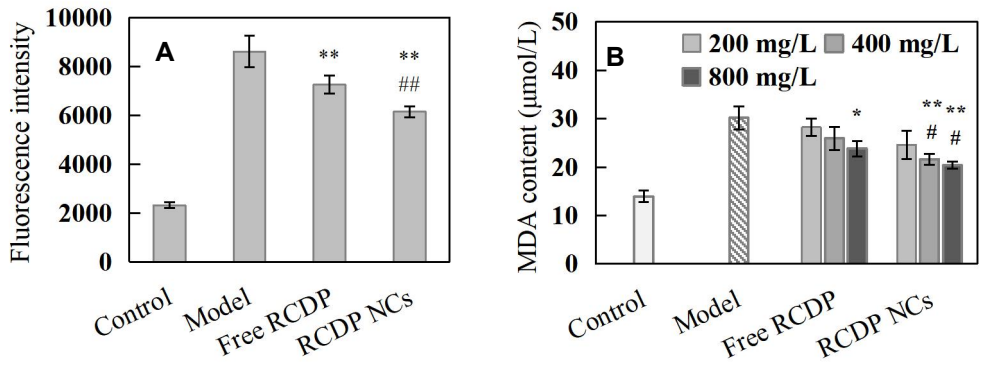

Figure 6. Oxidation indices of HSF cells, A. ROS; B. MDA content. (Note: Compared with Control, **P < 0.01, *P < 0.05; compared with Free RCDP, ##P < 0.01, #P < 0.05.)

3.6. β-galactosidase

The results of β-galactosidase staining in HSF cells treated with Free RCDP and RCDP NCs are presented in Figure 7.

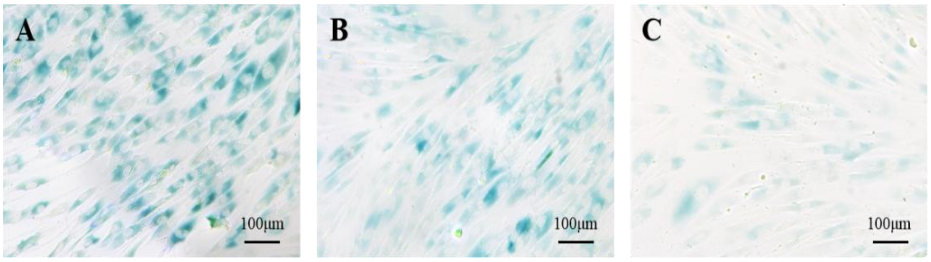

Figure 7. β-galactosidase staining of HSF cells (10X), A. Control group; B. Free RCDP group ; C. RCDP NCs group.

The 15th generation cells exhibited positive β-galactosidase staining, characterized by prominent dark blue coloration, indicating substantial cellular senescence. Following treatment with Free RCDP and RCDP NCs, the blue coloration of the cells was noticeably reduced. The treatment with RCDP NCs resulted in significantly lighter coloration compared to Free RCDP treatment, suggesting a more pronounced reduction in the senescent state of HSF cells after administration of RCDP NCs.

3.7. Autophagy-related proteins

The expression profiles of the autophagy-related proteins LC3I and LC3II, along with the degradation-related protein P62, determined by Western Blot analysis, are shown in Figure 8. As illustrated in Figure 8, the content of the autophagy-related protein P62 was significantly reduced in both the Free RCDP and RCDP NCs groups compared with the Control group ($P < 0.01$). Additionally, the ratio of the autophagy-related proteins LC3II/LC3I was substantially increased ($P < 0.01$). When compared with equivalent concentrations of Free RCDP, the RCDP NCs group exhibited a more pronounced decrease in P62 protein expression ($P < 0.01$) and a greater increase in the LC3II/LC3I ratio ($P < 0.01$). These findings demonstrate that RCDP NCs effectively enhance the autophagic capacity of HSF cells with superior efficacy compared to the free components.

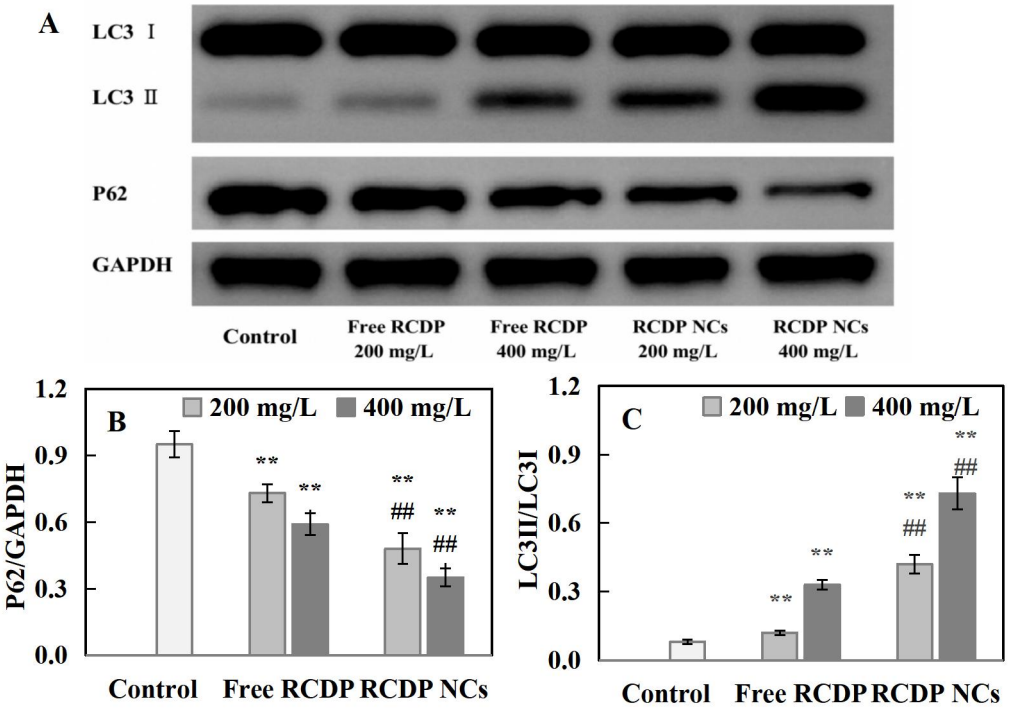

Figure 8. Expression of autophagy-related proteins in HSF cells. A. LC3I, LC3II, and P62 proteins; B. P62/GAPDH; C. LC3II/LC3I. (Note: Compared with Control, **P < 0.01; compared with Free RCDP, ##P < 0.01.)

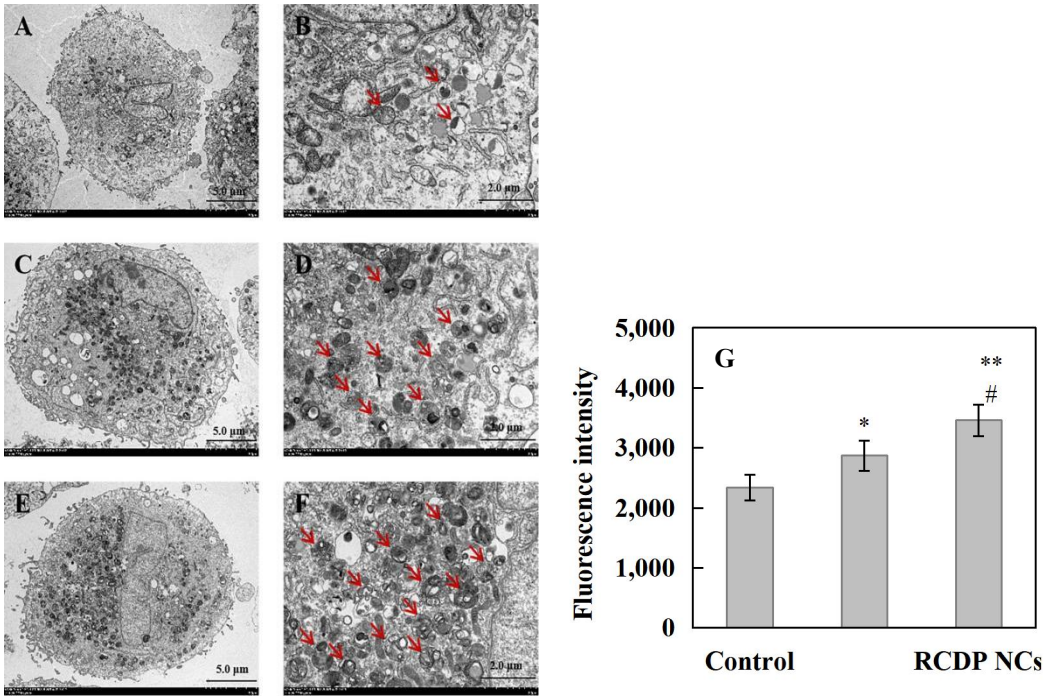

Figure 9. Autophagic lysosomes of HSF cells, A) Control group (2500×); B) Control group (7000×); C) Free RCDP group (2500×); D) Free RCDP group (7000×); E) RCDP NCs group (2500×); F) RCDP NCs group (7000×). The red arrows indicate autophagic lysosomes.G)Fluorescence intensity of MDC.(Note: Compared with Control, **P < 0.01,*P < 0.01; compared with the same concentration of Free RCDP, ##P < 0.01.)

3.8. Autophagosomes

Autophagosomes within cellular structures were visualized using transmission electron microscopy, with results presented in Figure 9.

As depicted in Figure 9, a few autophagosomes in cells from the Control group. In contrast, the cells treated with Free RCDP showed an increased presence of autophagosomes compared to the Control group. Notably, the highest density of autophagosomes was observed in the cytoplasm of cells treated with RCDP NCs. These microscopic findings further confirm that RCDP NCs enhance the autophagic capacity of HSF cells more effectively than free components.

3.9. MDC

MDC is an eosinophilic fluorescent pigment. In this study, it was used as a specific marker for detecting autophagosome formation. As shown in Figure 9G, compared with the control group, the average fluorescence intensity of MDC in both the Free RCDP group and RCDP NCs group was significantly higher. When compared to Free RCDP, RCDP NCs could significantly increase the average fluorescence intensity of MDC. These results indicate that RCDP NCs are more effective than Free RCDP in promoting autophagosome formation.

4. Discussion

Transdermal penetration assessments and cellular uptake investigations of RCDP NCs demonstrated that these carriers significantly enhanced the penetration efficiency, depth, and cellular utilization of the anti-aging compounds. Experimental results revealed that RCDP NCs reduced the content of ROS and MDA in the oxidative stress cell model. The observed decrease in MDA levels indicated that RCDP NCs inhibited oxidative stress reactions and minimized cellular damage. Furthermore, RCDP NCs decreased the content of the autophagy degradation-related protein p62, elevated the ratio of the autophagy-

related protein LC3II/LC3I, and increased autophagosome formation. During autophagy, p62 serves as a key ligating protein; it is selectively wrapped into the autophagosome and subsequently degraded by protein hydrolases in the autophagic lysosome. Its expression level negatively correlates with autophagic activity [18-21]. LC3I binds to autophagosome membranes and is converted into LC3II, so an increase in the LC3II/LC3I ratio indicates enhanced autophagy [22,23]. Through autophagy activation, RCDP NCs facilitated the clearance of damaged proteins and senescent organelles, thereby delaying cellular aging processes. Additionally, RCDP NCs stimulated proliferation in keratinocytes and fibroblasts, enhancing metabolic functions in aging skin. After treating 15 generations of HSF aging cells with RCDP NCs, a significant reduction in β-galactosidase—a cell aging biomarker—was observed, indicating a substantial improvement in cellular.

In this study, RCDP NCs primarily delayed cellular senescence through their potent antioxidant activity and autophagy promotion. The antioxidant properties enhanced inherent cellular defense mechanisms, mitigating damage to proteins, lipids, and organelles caused by reactive oxygen species and other free radicals. Autophagy functioned as a critical survival mechanism for aging cells responding to internal and external stressors. By eliminating damaged proteins and organelles, reducing oxidative stress-induced damage from various factors, and removing damaged proteins and senescent mitochondria among other organelles, RCDP NCs comprehensively delayed cellular senescence, promoted cellular proliferation, and retarded the progression of skin aging. Compared with previous studies on anti-aging active ingredients, this research not only explored the anti-aging mechanisms but also emphasized the efficient utilization of these compounds. These bioactive constituents are encapsulated within nanocarriers possessing a bilayer vesicular structure for optimized delivery. The efficiency optimization approach integrates enhancing bioavailability through penetration-promoting technology, achieving multi-mechanism coordination and synergistic anti-aging effects via scientific ingredient combinations, augmenting the stability of anti-aging active ingredients through nanocarrier encapsulation, preventing efficacy reduction through multidimensional optimization, and ultimately maximizing the cutaneous anti-aging effects of these active ingredients.

5. Conclusion

In this study, RCDP NCs penetrate deeper into the skin and are more effectively utilized by cells, significantly enhancing the transdermal delivery efficiency and bioavailability of RCDP. RCDP NCs exhibit strong antioxidant properties and autophagy regulation capabilities, thereby effectively delaying or even reversing aging effects. The research found that RCDP NCs promote cell proliferation while significantly reducing the levels of ROS and MDA, thus inhibiting oxidative stress damage. They also lower the expression of the autophagy degradation-related protein P62 and increase the LC3II/LC3I ratio, thereby enhancing autophagosome formation and effectively regulating cellular autophagy. RCDP NCs significantly improved cellular senescence, evidenced by a marked reduction in the senescence marker β-galactosidase. The antioxidant capacity, promotion of autophagy, and anti-aging effects of RCDP NCs surpass those of free RCDP at the same concentration. These findings provide strong evidence for using RCDP nanocarriers as functional ingredients in anti-aging cosmetic formulations, highlighting their significant potential in the cosmetics field.

6. References

[1] Warsito MF, Kusumawati I. The impact of herbal products in the prevention, regeneration and delay of skin aging. Adv. Exp. Med. Biol. 2019, 1178, 155-174.
[2] Zhao XJ, Hong YH, Liu W. Nanocarrier technology-from transdermal drug delivery to functional cosmetics. Detergent&Cosmetics. 2016, 44(7), 12-16.
[3] Martinez-Lopez N, Athonvarangku D, Singh R. Autophagy and aging. Adv. Exp. Med. Biol. 2015, 847, 73-87.

[4] Palmer DM, Kitchin JS. Oxidative damage, skin aging, antioxidants and a novel antioxidant rating system. J. Drugs. Dermatol. 2010, 9(1), 11-5.
[5] Gu Y, Han J, Jiang C, et al. Biomarkers, oxidative stress and autophagy in skin aging. Ageing. Res. Rev. 2020, 59, 101036.
[6] Mariño G, Niso-Santano M, Baehrecke EH, et al. Self-consumption: the interplay of autophagy and apoptosis. Nat. Rev. Mol. Cell. Biol. 2014, 15(2), 81-94.
[7] Roupe G. Skin of the aging human being. Lakartidningen, 2001, 98(10): 1091-1095.
[8] Muggleton-Harris AL, Defuria R. Age-dependent metabolic changes in cultured human fibroblasts. In Vitro Cell Dev. Biol. 1985, 21 (5), 271-276.
[9] Shecterle LM, St Cyr JA. Dermal benefits of topical D-ribose. Clin Cosmet Investig Dermatol. 2009, 2, 151-152.
[10] Wang J, Hu H, Wang J, et al. Characterization of recombinant humanized collagen type Ⅲ and its influence on cell behavior and phenotype. Collagen and Leather, 2023, 5(1), 84-96.
[11] Hua C, Zhu Y, Xu W, et al. Characterization by high-resolution crystal structure analysis of a triple-helix region of human collagen type III with potent cell adhesion activity. Biochem. Biophys. Res. Commun. 2019, 508(4), 018-1023.
[12] Baek JH, Kong US, Lee GM. Cosmetic composition for preventing skin wrinkles, containing carcinine(decarboxy carnosine 2HCl) having collagen synthetic and antioxidant effects: KR20030010259[P]. 2024-09-11.
[13] Yang F, Zhang X, Wang H, et al. Comprehensive evaluation of the efficacy and safety of a new multi-component anti-aging topical eye cream. Skin. Res. Technol. 2024, 30(7), e13790.
[14] Zhang S, Zhou H, Chen X, et al. Microneedle Delivery Platform Integrated with Codelivery Nanoliposomes for Effective and Safe Androgenetic Alopecia Treatment. ACS. Appl. Mater. Interfaces. 2024, 16(13), 15701-15717.
[15] Zhou H, Luo D, Chen D, et al. Current Advances of Nanocarrier Technology-Based Active Cosmetic Ingredients for Beauty Applications. Clin. Cosmet. Investig. Dermatol. 2021, 14, 867-887.
[16] Wang ZP, Shen HH, Luo D, et al. Preparation and efficacy evaluation of nanoliposomes for co-delivery of anti-alopecia agents. Chin. Surf. Deter. Cos. 2020, 50(6), 396-401.
[17] Kim, B. S, Na, Y. G, Choi, J. H, et al. The Improvement of Skin Whitening of Phenylethyl Resorcinol by Nanostructured Lipid Carriers. Nanomaterials (Basel). 2017, 7(9): 241.
[18] Misovic M, Milenkovic D, Martinovic T, et al. Short-term exposure to UV-A, UV-B, and UV-C irradiation induces alteration in cytoskeleton and autophagy in human keratinocytes. Ultrastruct. Pathol. 2013, 37(4), 241-248.
[19] Jung CH, Ro SH, Cao J, et al. mTOR regulation of autophagy. FEBS. Lett. 2010, 584(7), 1287-1295.
[20] Klionsky DJ, Emr SD. Autophagy as a regulated pathway of cellular degradation. Science. 2000, 290(5497), 1717-1721.
[21] Alotaibi MR, As SH, Alaqil FA, et al. A newly synthesizedplatinum-based compound (PBC-Ⅱ) increases chemosensitivity of HeLa ovarian cancer cells via inhibition of autophagy. Saudi. Pharm. J. 2019, 27(8), 1203-9.
[22] Chen SM, Gong YC, Sui L, et al. Role of tangeretin on autoph-agy in human gastric cancer AGS cells and its mechanism. Chin. Pharmacol. Bull. 2019, 35(12), 1671-6.
[23] Qi M, Tan BE. Molecular mechanism of autophagy regulating oxidative stress in animals. Chin. J. Anim. Nut. 2020, 32(9), 10.